



Imidazolone–amide bridges and their effects on tubulin polymerization in *cis*-locked vinylogous combretastatin-A4 analogues: Synthesis and biological evaluation

Yao-Wu Li^{b,†}, Jia Liu^{a,†}, Na Liu^a, Duo Shi^a, Xiao-Tian Zhou^a, Jia-Guo Lv^a, Ju Zhu^a, Can-Hui Zheng^{a,*}, You-Jun Zhou^{a,*}

^aSchool of Pharmacy, Second Military Medical University, Shanghai 200433, China

^bAir Force General Hospital, Beijing 100036, China

ARTICLE INFO

Article history:

Received 11 February 2011

Revised 27 March 2011

Accepted 30 March 2011

Available online 3 April 2011

Keywords:

Imidazolone–amide

Tubulin polymerization inhibitor

Antitumor agent

ABSTRACT

A series of novel combretastatin-A4 analogues in which the *cis*-olefinic bridge is replaced by an imidazolone–amide were synthesized, and their cytotoxicity and tubulin-polymerization inhibitory activities were evaluated. These compounds appear to be potential tubulin-polymerization inhibitors. Compounds **10**, **9b** and **9c**, bearing 3'-NH₂-4'-OCH₃, 4'-CH₃ and 3'-CH₃-substituted 1-phenyl B-ring, confer optimal bioactivity. The binding modes of these compounds to tubulin were obtained by molecular docking, which can explain the compounds' structure–activity relationship. The studies presented here provide a new structural type for the development of novel antitumor agents.

© 2011 Elsevier Ltd. All rights reserved.

1. Introduction

Microtubule polymerization dynamics can greatly affect a cell's ability to change and maintain its shape and undergo critical processes such as cell signaling and mitosis. At the same time, these polymerization dynamics can be profoundly affected by even small chemical changes.¹ For this reason, microtubules are attractive molecular targets for anticancer therapeutics. Three distinct microtubule small-molecule binding sites are well characterized. These include the vinca, taxane and colchicine sites. The colchicine site is located on monomeric unpolymerized α/β -tubulin, and inhibitors that bind to tubulins at this site disrupt the polymerization of tubulin into microtubules.²

Natural products are an important source of colchicine site inhibitors (CSIs). The first colchicine site inhibitor (CSI), colchicine (Scheme 1), was extracted from the poisonous meadow saffron *Colchicum autumnale* L, but its high toxicity has limited its therapeutic applications.³ Combretastatin A-4 (CA-4) (Scheme 1), isolated from a South African willow tree *Combretum caffrum*, binds to the colchicine site and exerts potent cytotoxicity against

a wide variety of human cancer cell lines including MDR cancer cell lines. Unfortunately, CA-4 does not show efficacy *in vivo* because of its low aqueous solubility and the isomerization of its *cis*-double bond into the more thermally stable, but inactive, *trans*-isomer.⁴ However, a more soluble prodrug, CA-4 phosphate disodium (CA-4P), has displayed promising results in human cancer clinical trials,⁵ thus fueling continued research in novel CA-4 analogues.

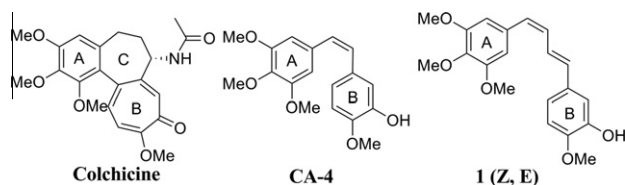
Over the years, a large number of natural and synthetic CA-4 analogues have been identified as CSIs.^{2,4–6} However, only a few of these have been found to have linkers of three or more atoms between the two aryl rings of the acyclic bridgehead.^{7–10} Ty et al. reported that the vinylogous analogues of CA-4, **1** (Scheme 1) and its (*E*, *Z*)-dienic isomer show comparable tubulin polymerization inhibitory activity with CA-4. However, these dienic derivatives are prone to isomerization and become more stable but inactive (*E*, *E*)-isomeric derivatives.¹¹ The cyclopropyl group is generally considered an alkene bioisostere, and a secondary amide may be considered to have a similar spatial disposition to that of a *trans*-alkene. Under such context, a type of configurationally *cis*-locked vinylogous CA-4 analogues, characterized by a cyclopropyl–amide unit (structure B in Scheme 2) was synthesized. However, these compounds showed low tubulin polymerization inhibition and cytotoxic activity,¹² which may be related to the spatial difference between the cyclopropyl and the *cis*-alkene group. To solve the problem, we first wanted to evaluate a number of amide derivatives whose cyclopropyl group was replaced by a group more spatially similar to *cis*-alkene. Because five-membered

Abbreviations: CSI, colchicine site inhibitor; CA-4, combretastatin A-4; CA-4P, CA-4 phosphate disodium; TMP, trimethoxyphenyl.

* Corresponding authors. Tel.: +86 021 81871240 (C.-H.Z.); tel.: +86 021 81871231 (Y.-J.Z.).

E-mail addresses: canhui_zheng@yahoo.com.cn (C.-H. Zheng), zhouyoujun2006@yahoo.com.cn (Y.-J. Zhou).

[†] These authors contributed equally to this work.



Scheme 1. Two-dimensional structures of three colchicine site inhibitors.

heterocycle has been shown to be a good surrogate for the double bond of CA-4 with regards to retaining the *cis*-alkene configuration,^{4–6} it seems likely that CA-4 analogues bearing a five-membered heterocycle–amide moiety (structure C in Scheme 2) will confer good bioactivity and improve physicochemical properties. In this study, a series of *cis*-locked vinylogous CA-4 analogues characterized by a imidazolone–amide unit were synthesized, and the cytotoxicity and tubulin-polymerization inhibitory activity of each analogue was evaluated. Their modes of binding to tubulin were studied by molecular docking.

2. Results and discussion

2.1. Synthesis

The chemical synthesis of these compounds is outlined in Scheme 3. Compounds 2–7 was obtained by our previous procedure.¹³ Intermediate 2 was prepared in 82.6% yield by treatment of 3,4,5-trimethoxybenzoic acid with SOCl_2 . Compound 2 was treated with $\text{CH}_3\text{COCH}_2\text{COOC}_2\text{H}_5$ and $\text{C}_2\text{H}_5\text{ONa}$ in $\text{C}_2\text{H}_5\text{OH}$ to afford 3 in

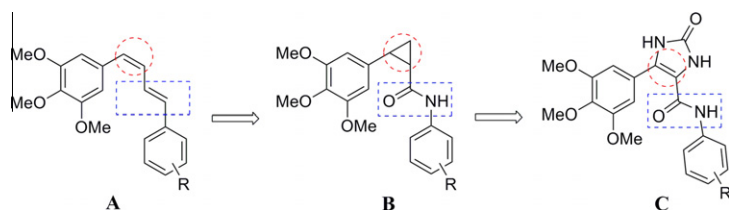
76.7% yield. Decarboxylation of 3 by NH_4OH provided intermediate 4 in 78.2% yield. Compound 4 was treated with NBS in diethyl ether to provide 5 in 88.2% yield. Then 5 was allowed to react with $\text{CO}(\text{NH}_2)_2$ in $\text{N}(\text{C}_2\text{H}_5)_3/\text{DMF}$ to form the products of cyclization 6 in 62.8% yield. Hydrolysis of 6 by $\text{NaOH}/\text{H}_2\text{O}$ yielded 7 in 81.5% yield. The resulting compound 7 was allowed to react with different aromatic amine compounds 8(a–m) and 1-naphthylamine by EDC/DMAP in DMF to yield 9(a–m) and 11 in medium yield. Reduction of 9m with SnCl_2/HCl in water provided 10 in 49% yield. The structures of the target compounds are reported in Table 1.

2.2. Biological evaluation

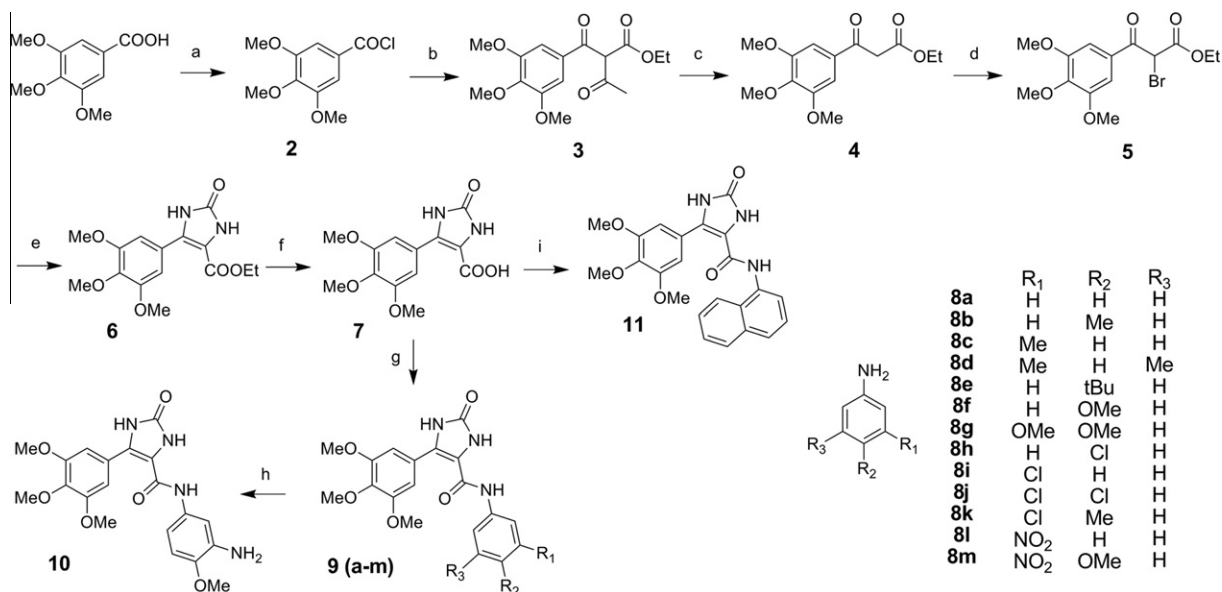
The cytotoxicity of compounds 9(a–m), 10, and 11 were evaluated against three human tumor cell lines by MTT assay: the CEM human leukemia, MDA-MB-435 human breast carcinoma and LOVO human colon carcinoma cell lines. The cytotoxicity levels of the target compounds are reported in Table 1.

CA-4 analogues with imidazolone–amide bridges showed more cytotoxic activity than CA-4 analogues with cyclopropyl–amide bridges.¹² Compound 10, which has a substitution pattern similar to that of CA-4 and neoflavonoid derivative 1, demonstrated strong cytotoxicity. Compounds 9b and 9c also showed strong cytotoxicity. Middle to low cytotoxic effects were observed with 9a, 9(d–g), 9(i–k) and 11.

The characteristics of the 1-phenyl B-ring (Table 1) are important for the cytotoxic efficacy of these compounds. A 4'-hydrophobic group on the 1-phenyl B-ring increases cytotoxic activity. This is evidenced by compounds 9b, 9e and 9f, which each has a 4'- CH_3 ,

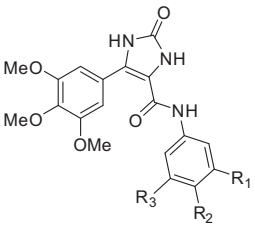
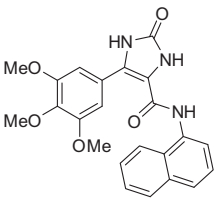


Scheme 2. Design concept of new configurationally *cis*-locked vinylogous CA-4 analogues.



Scheme 3. Synthesis of CA-4 analogues with an imidazolone–amide bridge. Reagents and conditions: (a) SOCl_2 , 75 °C; (b) $\text{CH}_3\text{COCH}_2\text{COOC}_2\text{H}_5/\text{C}_2\text{H}_5\text{ONa}$, rt; (c) NH_4OH , rt; (d) NBS/ $\text{C}_2\text{H}_5\text{OC}_2\text{H}_5$, rt; (e) $\text{CO}(\text{NH}_2)_2/\text{N}(\text{C}_2\text{H}_5)_3/\text{DMF}$, 80 °C; (f) $\text{NaOH}/\text{H}_2\text{O}$, 55 °C; (g) 8(a–m)/EDC/DMAP/DMF, rt; (h) $\text{SnCl}_2/\text{HCl}/\text{H}_2\text{O}/80$ °C; (i) 1-naphthylamine/EDC/DMAP/DMF, rt.

Table 1
Cytotoxicity of subject compounds

No.	Compound structure			Cytotoxicity (IC ₅₀ , μ M)		
	R ₁	R ₂	R ₃	CEM	MDA-MB-435	LOVO
9a	H	H	H	45.87	40.37	77.64
9b	H	Me	H	0.24	0.63	4.67
9c	Me	H	H	0.18	0.76	0.62
9d	Me	H	Me	19.43	33.78	23.45
9e	H	tBu	H	38.83	32.21	33.99
9f	H	OMe	H	2.30	17.43	35.60
9g	OMe	OMe	H	4.19	4.87	11.90
9h	H	Cl	H	>200	151.91	110.44
9i	Cl	H	H	4.80	4.77	3.62
9j	Cl	Cl	H	12.09	19.23	4.93
9k	Cl	Me	H	2.11	8.34	5.46
9l	NO ₂	H	H	>200.0	44.23	35.02
9m	NO ₂	OMe	H	>200.0	>240	43.92
10	NH ₂	OMe	H	0.33	0.62	3.4
11	/	/	/	11.87	9.32	3.46
						
						
Colchicine	/	/	/	0.0172	0.0073	0.101

4'-OCH₃ and 4'-tBu substituted 1-phenyl B-ring. These three compounds are more active than **9a** and **9h**, which have 4'-unsubstituted and 4'-Cl substituted 1-phenyl B-rings. Based on the comparison of their cytotoxic activities, methyl may be the optimal group for this position. Another important factor that affects cytotoxicity is the 3' position of the 1-phenyl B-ring. In this position, several small-size polar and nonpolar groups increase cytotoxic activity. This is evidenced by compounds **9c** and **9i**, which each has a 3'-CH₃ and 3'-Cl substituted 1-phenyl B-ring and becomes more active than 3'-unsubstituted **9a**, and by compounds **10** and **9g**, which have 3'-NH₂-4-OCH₃- and 3'-OCH₃-4-OCH₃-substituted 1-phenyl B-rings and are more active than 3'-unsubstituted-4-OCH₃ compound **9f**. However, compounds with larger-sized 3'-NO₂, are significantly unfavorable to the cytotoxic activity. The 3'-NO₂-substituted compounds **9l** and **9m** show significantly less activity.

To test whether these compounds bind to tubulin and inhibit its polymerization, representative compounds **10**, **9b**, **9c** and **9m** were subjected to evaluation by tubulin assembly assay. CA-4 was also evaluated by this assay as a positive control. Figure 1 shows the effects of these compounds in 10 μ M solution on the turbidimetry time course of microtubule assembly from pure tubulin. The final amount of microtubule was significantly lower in the presence of **10**, **9b** and **9c** than in the blank control experiment, and the extent of inhibition by these compounds was about half of that of CA-4. However, the inhibition activity level of compound **9m** was significantly lower than that of **10**, **9b** or **9c**. It showed almost no effect on tubulin polymerization in 10 μ M solution. Considering that compounds **10**, **9b** and **9c**, which each showed strong cytotoxicity, clearly inhibited tubulin assembly, while **9m**, which showed little cytotoxicity, had very little effect in this assay, it seems that tubulin represents a potential target for CA-4 analogues with an imidazolone–amide bridge.

Because the inhibition of tubulin polymerization has implicated in G₂/M phase cell cycle arrest in various cancer cell lines,^{14–16} the effects of compound **10** on the cell cycle progression on LOVO cells was determined (Fig. 2). The results of flow cytometry analysis indicate **10** induce a modest accumulation of cells in the G₂/M phase (28% compared to 13% for untreated cells) in 5 μ M (Fig. 2B), and cause a more evident accumulation (74%) in a higher concentration 25 μ M (Fig. 2C).

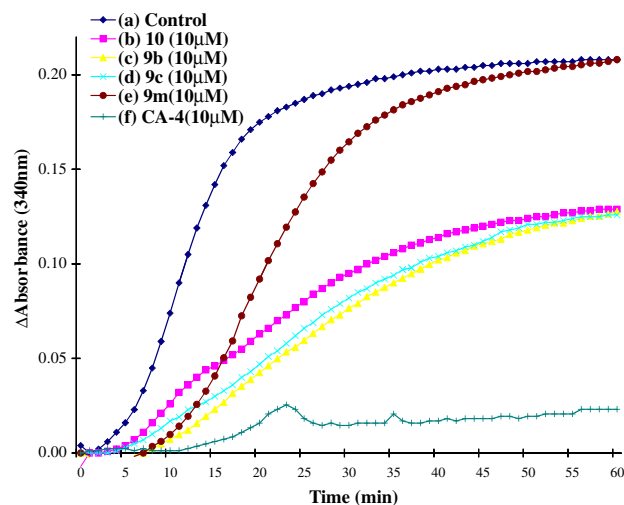


Figure 1. Effect of subject compounds on the turbidity time course of in vitro microtubule assembly. The reaction was started by warming the solution from 0 to 37 °C. The figure shows (a) tubulin at 3 mg/mL and (b–f) aliquots of the same solution with 10 μ M of **10**, **9b**, **9c**, **9m** and CA-4, respectively.

To validate the observed structure–activity relationships, molecular docking studies of the vinylogous analogues of CA-4, **1** and CA-4 analogues with an imidazolone–amide bridge to tubulin protein were performed. The X-ray crystal structure of the DAMA-colchicine-tubulin complex (PDB code 1SA0) was used as the tubulin protein template. Based on the predictive binding modes of **1** (Fig. 3B) and **10** (Fig. 3C) to tubulin, the imidazolone–amide bridge of **10** retains the (Z, E)-dienic configuration of **1** well, which is consistent with our design concept. The bridge moieties cause the A-ring and B-ring of these compounds to lie in similar positions to that of the colchicine site with colchicines, whose binding mode is derived from X-ray crystal structure 1SA0 (Fig. 3A). The A-ring trimethoxyphenyl (TMP) moiety of **10** can foster Van der Waals interactions with the hydrophobic P1 pocket in the interface between α/β -tubulin. The –OCH₃ substituted on it can form a hydrogen bond with Cys241 in β subunit. The 1-phenyl B-ring of

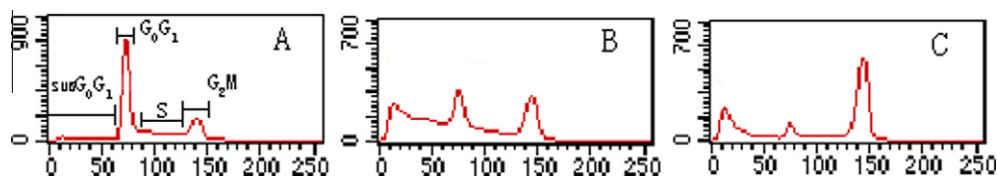


Figure 2. Cell cycle distribution determined by flow cytometry on LOVO cells treated for 24 h without any compounds (A) or with compound **10** in 5 μ M (B) and 25 μ M (C). Sub-G₀-G₁, G₀-G₁, S, and G₂-M cells are indicated in the panel (A).

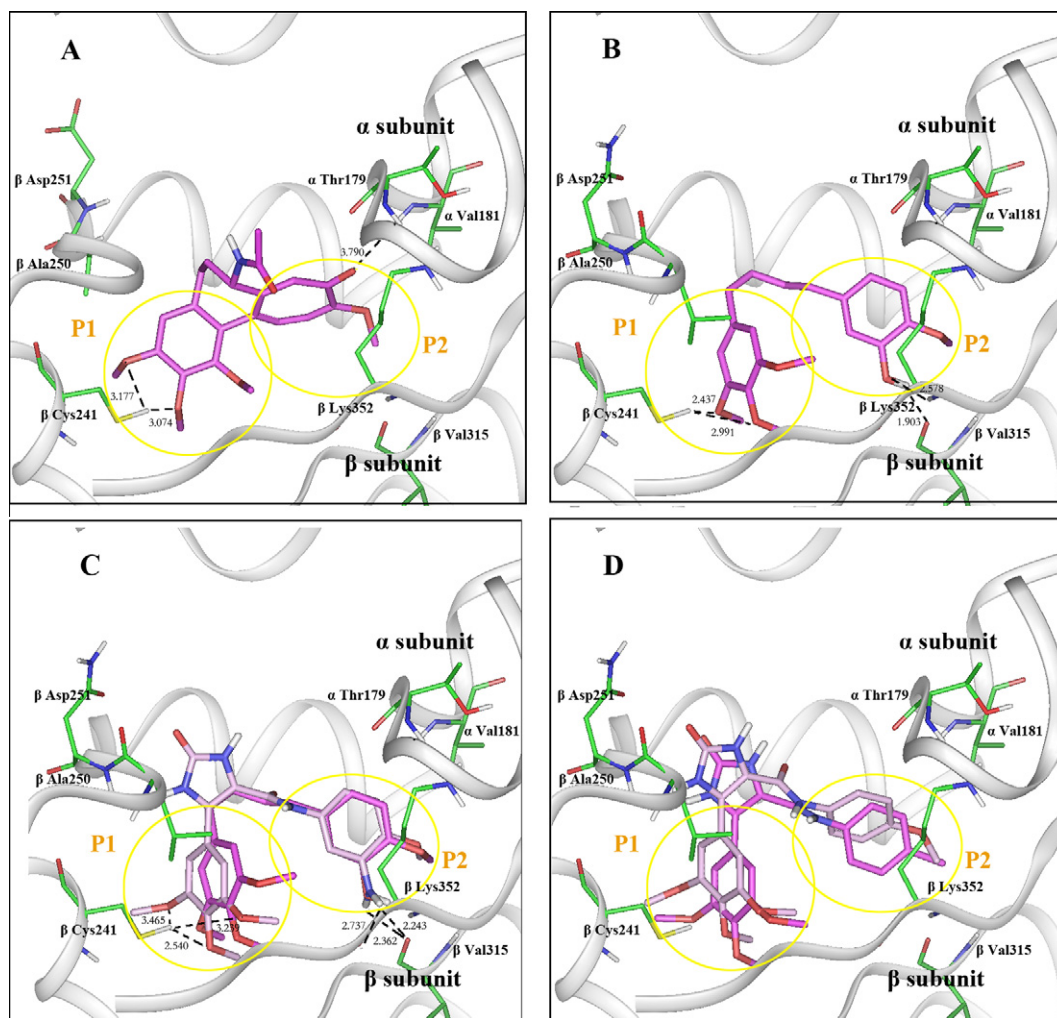


Figure 3. Binding modes of colchicine (A) and **1** (B) to tubulin protein and the comparison between the binding modes of **1** (purple in C), **10** (light purple in C), **9b** (purple in D) and **9f** (light purple in D). The binding mode of colchicine is derived from the X-ray crystal structure of the DAMA-colchicine-tubulin complex (PDB code 1SA0). P1 and P2 are two hydrophobic pockets in the interface between α/β -tubulin. The black dot lines denote the distance between two atoms (Å).

10 and 4'-OCH₃ on it can foster Van der Waals interactions with the hydrophobic P2 pocket, which can explain why the 4'-hydrophobic group on the 1-phenyl B-ring is favorable to cytotoxic activity. On the basis of the comparison between the binding modes of **9b** and **9f** (Fig. 3D), the compound bearing 4'-CH₃ 1-phenyl B-ring binds into the colchicine site deeper than when it bears 4'-OCH₃, which may explain why methyl may be the optimal group for this position. 3'-NH₂ substituted on the 1-phenyl B-ring of **10** can form hydrogen bonds with the backbone at Val315 and Lys352 in β subunit. However, this group still lies in a hydrophobic position with limited space, which can explain why several small-size polar and nonpolar groups are favorable to cytotoxic activity while the 3'-NO₂ group of larger size is not.

3. Conclusion

This paper describes the synthesis of a series of novel combretastatin-A4 analogues, in which the *cis*-olefinic bridge is replaced by an imidazolone–amide, and the evaluation of their cytotoxicity and tubulin polymerization inhibitory activity. These compounds seem to show promise as potential tubulin polymerization inhibitors. Compounds **10**, **9b** and **9c**, bearing 3'-NH₂-4'-OCH₃-, 4'-CH₃- and 3'-CH₃-substituted 1-phenyl B-rings, confer optimal bioactivity. The binding modes of these compounds to tubulin protein were obtained by molecular docking, which explains the structure–activity relationships. The studies presented here provide a new structural type for the development of novel antitumor agents.

4. Experiments

4.1. Chemistry

Melting points were determined on an electrically heated RK-Z melting point apparatus and are uncorrected. Mass spectra (MS) were measured on a Micromass Qtof-Micro LC-MS instrument. ^1H NMR spectra were recorded at 300 MHz on a Bruker AC-300P spectrometer with Me₄Si as the internal standard. Chemical shifts are given in ppm (δ), and the spectral data are consistent with the assigned structures. Silica gel column chromatography was performed with Silica gel 60 G (Qindao Haiyang Chemical, China). Commercial solvents and reagents were of reagent grade and, when necessary, were purified and dried by standard protocols. Organic solutions were dried over anhydrous sodium sulfate. Compounds **2–7** was obtained by our previous procedure.¹³

4.1.1. General procedure for the preparation of **9(a–m)**, **11**

A mixture of **7** (0.02 mol), **8(a–m)** or 1-naphthylamine (0.02 mol), EDC (0.08 mol), DMAP (0.002 mol) and DMF (60 ml) was stirred at room temperature for 12 h. Then water (200 ml) was added, and the resulting solid was filtered and washed by water twice. After filtration, the filter cake was recrystallized to yield compounds **9(a–m)** and **11** (30–60%).

4.1.1.1. 2-Oxo-N-Phenyl-5-(3,4,5-trimethoxyphenyl)-2,3-dihydro-1H-imidazole-4-carboxamide (9a). Light yellow crystal: mp 216–219 °C; ^1H NMR (300 MHz, DMSO, δ ppm): 3.69 (s, 3H, Ar–OCH₃), 3.72 (s, 6H, Ar–OCH₃), 7.08 (d, 1H, J = 9 Hz, Ar–H), 7.29–7.35 (m, 2H, Ar–H), 7.42 (br, 2H, imidazolone-NH), 7.67 (d, 2H, J = 9 Hz, Ar–H), 7.69 (s, 2H, Ar–H), 9.74 (s, 1H, Ar–NHCO); ESI-MS (m/z): 370.41 [$M+H$]⁺.

4.1.1.2. 2-Oxo-N-p-Tolyl-5-(3,4,5-trimethoxyphenyl)-2,3-dihydro-1H-imidazole-4-carboxamide (9b). Light yellow crystal: mp 224–226 °C; ^1H NMR (300 MHz, DMSO, δ ppm): 2.25 (s, 3H, Ar–CH₃), 3.69 (s, 3H, Ar–OCH₃), 3.77 (s, 6H, Ar–OCH₃), 7.12 (d, 2H, J = 8.4 Hz, Ar–H), 7.41 (br, 2H, imidazolone-NH), 7.56 (d, 2H, J = 8.4 Hz, Ar–H), 7.69 (s, 2H, Ar–H), 9.66 (s, 1H, Ar–NHCO); ESI-MS (m/z): 384.45 [$M+H$]⁺.

4.1.1.3. 2-Oxo-N-m-Tolyl-5-(3,4,5-trimethoxyphenyl)-2,3-dihydro-1H-imidazole-4-carboxamide (9c). Light yellow crystal: mp 205–207 °C; ^1H NMR (300 MHz, CDCl₃, δ ppm): 2.36 (s, 3H, Ar–CH₃), 3.91 (s, 3H, Ar–OCH₃), 3.94 (s, 6H, Ar–OCH₃), 5.38 (br, 2H, imidazolone-NH), 6.95–6.97 (m, 1H, Ar–H), 7.21–7.24 (m, 1H, Ar–H), 7.35–7.42 (m, 2H, Ar–H), 7.58 (s, 2H, Ar–H), 7.76 (s, 1H, Ar–NHCO); ESI-MS (m/z): 384.49 [$M+H$]⁺.

4.1.1.4. N-(3,5-Dimethylphenyl)-2-oxo-5-(3,4,5-trimethoxyphenyl)-2,3-dihydro-1H-imidazole-4-carboxamide (9d). Light yellow crystal: mp 215–218 °C; ^1H NMR (300 MHz, CDCl₃, δ ppm): 6.06 (s, 6H, Ar–CH₃), 3.90 (s, 3H, Ar–OCH₃), 3.93 (s, 6H, Ar–OCH₃), 5.21 (br, 2H, imidazolone-NH), 6.78 (s, 1H, Ar–H), 7.20 (s, 2H, Ar–H), 7.51 (s, 2H, Ar–H), 7.68 (s, 1H, Ar–NHCO); ESI-MS (m/z): 398.38 [$M+H$]⁺.

4.1.1.5. N-(4-Tert-butylphenyl)-2-oxo-5-(3,4,5-trimethoxyphenyl)-2,3-dihydro-1H-imidazole-4-carboxamide (9e). Light yellow crystal: mp 202.5–204 °C; ^1H NMR (300 MHz, DMSO, δ ppm): 1.26 (s, 9H, *tert*-butyl), 3.69 (s, 3H, Ar–OCH₃), 3.78 (s, 6H, Ar–OCH₃), 7.33 (d, 2H, J = 8.7 Hz, Ar–H), 7.38 (br, 2H, imidazolone-NH), 7.58 (d, 2H, J = 8.7 Hz, Ar–H), 7.70 (s, 2H, Ar–H), 9.65 (s, 1H, Ar–NHCO); ESI-MS (m/z): 472.40 [$M+H$]⁺.

4.1.1.6. N-(4-Methoxyphenyl)-2-oxo-5-(3,4,5-trimethoxyphenyl)-2,3-dihydro-1H-imidazole-4-carboxamide (9f). Brown crystal: mp 228–229 °C; ^1H NMR (300 MHz, DMSO, δ ppm): 3.68 (s, 3H, Ar–OCH₃), 3.72 (s, 3H, Ar–OCH₃), 3.77 (s, 6H, Ar–OCH₃), 6.90 (d, 2H, J = 9 Hz, Ar–H), 7.36 (br, 2H, imidazolone-NH), 7.58 (d, 2H, J = 9 Hz, Ar–H), 7.7 (s, 2H, Ar–H), 9.64 (s, 1H, Ar–NHCO); ESI-MS (m/z): 400.40 [$M+H$]⁺.

4.1.1.7. N-(3,4-Dimethoxyphenyl)-2-oxo-5-(3,4,5-trimethoxyphenyl)-2,3-dihydro-1H-imidazole-4-carboxamide (9g). Light yellow crystal: mp 216–218 °C; ^1H NMR (300 MHz, DMSO, δ ppm): 3.69 (s, 3H, Ar–OCH₃), 3.72 (s, 6H, Ar–OCH₃), 3.78 (s, 6H, Ar–OCH₃), 6.90 (d, 1H, J = 8.7 Hz, Ar–H), 7.26–7.32 (m, 2H, Ar–H), 7.37 (br, 2H, imidazolone-NH), 7.69 (s, 2H, Ar–H), 9.60 (s, 1H, Ar–NHCO); ESI-MS (m/z): 430.46 [$M+H$]⁺.

4.1.1.8. N-(4-Chlorophenyl)-2-oxo-5-(3,4,5-trimethoxyphenyl)-2,3-dihydro-1H-imidazole-4-carboxamide (9h). White crystal: mp 240 °C, dec.; ^1H NMR (300 MHz, DMSO, δ ppm): 3.69 (s, 3H, Ar–OCH₃), 3.78 (s, 6H, Ar–OCH₃), 7.37 (d, 2H, J = 9 Hz, Ar–H), 7.45 (br, 2H, imidazolone-NH), 7.69 (s, 2H, Ar–H), 7.73 (d, 2H, J = 9 Hz, Ar–H), 9.91 (s, 1H, Ar–NHCO); ESI-MS (m/z): 402.36 [$M+H$]⁺.

4.1.1.9. N-(3-Chlorophenyl)-2-oxo-5-(3,4,5-trimethoxyphenyl)-2,3-dihydro-1H-imidazole-4-carboxamide (9i). Light yellow crystal: mp 207–208 °C; ^1H NMR (300 MHz, CDCl₃, δ ppm): 3.91 (s, 3H, Ar–OCH₃), 3.93 (s, 6H, Ar–OCH₃), 5.47 (br, 2H, imidazolone-NH), 7.10–7.13 (m, 1H, Ar–H), 7.25–7.30 (m, 1H, Ar–H), 7.39–7.44 (m, 1H, Ar–H), 7.59 (s, 2H, Ar–H), 7.73 (s, 1H, Ar–H), 7.84 (s, 1H, Ar–NHCO); ESI-MS (m/z): 404.38 [$M+H$]⁺.

4.1.1.10. N-(3,4-Dichlorophenyl)-2-oxo-5-(3,4,5-trimethoxyphenyl)-2,3-dihydro-1H-imidazole-4-carboxamide (9j). Brown crystal: mp 209–211 °C; ^1H NMR (300 MHz, DMSO, δ ppm): 3.70 (s, 3H, Ar–OCH₃), 3.78 (s, 6H, Ar–OCH₃), 7.47 (br, 2H, imidazolone-NH), 7.56–7.71 (m, 5H, Ar–H), 8.04 (s, 1H, Ar–NHCO); ESI-MS (m/z): 438.41 [$M+H$]⁺.

4.1.1.11. N-(3-Chloro-4-methylphenyl)-2-oxo-5-(3,4,5-trimethoxyphenyl)-2,3-dihydro-1H-imidazole-4-carboxamide (9k). Light yellow crystal: mp 233–235 °C; ^1H NMR (300 MHz, DMSO, δ ppm): 2.27 (s, 3H, Ar–CH₃), 3.69 (s, 3H, Ar–OCH₃), 3.78 (s, 6H, Ar–OCH₃), 7.28 (d, 1H, J = 6.3 Hz, Ar–H), 7.43 (br, 2H, imidazolone-NH), 7.52 (dd, 1H, J_1 = 6.3 Hz, J_2 = 2.1 Hz, Ar–H), 7.66 (s, 2H, Ar–H), 7.83 (d, J = 2.1 Hz, 1H, Ar–H), 9.86 (s, 1H, Ar–NHCO); ESI-MS (m/z): 418.65 [$M+H$]⁺.

4.1.1.12. N-(3-Nitrophenyl)-2-oxo-5-(3,4,5-trimethoxyphenyl)-2,3-dihydro-1H-imidazole-4-carboxamide (9l). Yellow crystal: mp 240 °C, dec.; ^1H NMR (300 MHz, DMSO, δ ppm): 3.70 (s, 3H, Ar–OCH₃), 3.79 (s, 6H, Ar–OCH₃), 7.49 (br, 2H, imidazolone-NH), 7.62 (t, 2H, J = 8.4 Hz, Ar–H), 7.67 (s, 2H, Ar–H), 7.90–7.94 (m, 1H, J = 8.4 Hz, Ar–H), 8.13 (d, 1H, J = 7.8 Hz, Ar–H), 8.69 (t, 1H, J = 2.1 Hz, Ar–H); ESI-MS (m/z): 413.42 [$M+H$]⁺.

4.1.1.13. N-(4-Methoxy-3-nitrophenyl)-2-oxo-5-(3,4,5-trimethoxyphenyl)-2,3-dihydro-1H-imidazole-4-carboxamide (9m). Yellow crystal: mp 223–225 °C; ^1H NMR (300 MHz, DMSO, δ ppm): 3.69 (s, 3H, Ar–OCH₃), 3.78 (s, 6H, Ar–OCH₃), 3.90 (s, 3H, Ar–OCH₃), 7.37 (d, 1H, J = 9.3 Hz, Ar–H), 7.45 (br, 2H, imidazolone-NH), 7.67 (s, 2H, Ar–H), 7.93 (dd, 1H, J_1 = 9.3 Hz, J_2 = 2.7 Hz, Ar–H), 8.29 (d, 1H, J = 2.7 Hz, Ar–H), 10.03 (s, 1H, Ar–NHCO); ESI-MS (m/z): 445.42 [$M+H$]⁺.

4.1.1.14. N-(Naphthalen-1-yl)-2-oxo-5-(3,4,5-trimethoxyphenyl)-2,3-dihydro-1H-imidazole-4-carboxamide (11). Brown crystal: mp 202–203 °C; ¹H NMR (300 MHz, DMSO, δ ppm): 3.70 (s, 3H, Ar-OCH₃), 3.79 (s, 6H, Ar-OCH₃), 7.40–7.47 (m, 2H, Ar-H), 7.44 (br, 2H, imidazolone-NH), 7.69 (s, 2H, Ar-H), 7.73–7.79 (m, 1H, Ar-H), 7.81–7.88 (m, 3H, Ar-H), 8.30 (d, 1H, J = 2.1 Hz, Ar-H), 9.94 (s, 1H, Ar-NHCO); ESI-MS (m/z): 421.00 [M+H]⁺.

4.1.2. N-(3-Amino-4-methoxyphenyl)-2-oxo-5-(3,4,5-trimethoxyphenyl)-2,3-dihydro-1H-imidazole-4-carboxamide (10)

Compound **8m** (2 g) was added into a solution of SnCl₂ (4.1 g) in hydrochloric acid (40 ml), and the reaction mixture was stirred at 80 °C for 4 h. After cooling, the pH value of the reaction mixture was adjusted to 8 by sodium hydroxide. Then the solution was extracted with acetic ether and dried over Na₂SO₄. Distillation of the solvent under reduced pressure and recrystallization of the residue yielded compounds **10** (0.92 g, 49%) as brown crystal (49% yield): mp 200–202 °C; ¹H NMR (300 MHz, DMSO, δ ppm): 2.27 (s, 3H, Ar-CH₃), 3.69 (s, 3H, Ar-OCH₃), 3.78 (s, 6H, Ar-OCH₃), 4.77 (br, 2H, NH₂), 6.69–7.75 (m, 2H, Ar-H), 7.00 (d, 1H, J = 2.1 Hz, Ar-H), 7.33 (br, 2H, imidazolone-NH), 7.68 (s, 2H, Ar-H), 9.33 (s, 1H, Ar-NHCO); ESI-MS (m/z): 418.65 [M+H]⁺.

4.2. Biology

4.2.1. In vitro cytotoxicity assay

Cytotoxic effects were examined in the CEM human leukemia, MDA-MB-435 human breast carcinoma, and LOVO human colon carcinoma cell lines. Cells in logarithmic phase were diluted to a density of 40000–50000 cells/mL in culture medium based on growth characteristics. For each well of a 96-well microplate, 100 μ L of cell dilution was seeded, allowed to attach overnight, and then exposed to varying concentrations (10^{−4}–10^{−9} M) of compounds for 72 h (37 °C, 5% CO₂ atmosphere). The number of living cells was estimated by the MTT assay. Absorbance at 570 nm was recorded on a Wellsan MK-2 multifunction microplate reader (Labsystems Inc.). Compounds were tested in triplicate in at least three independent assays. The IC₅₀ values were determined by a nonlinear regression analysis. Average values were reported.

4.2.2. In vitro tubulin polymerization assay^{16–18}

Bovine brain tubulin was purchased from cytoskeleton. Tubulin (>99% pure, 3 mg/mL) in 100 μ L of general tubulin buffer (80 mM Na-pipes, pH 6.9, 1 mM EGTA, 1 mM MgCl₂, 1 mM GTP, and 5% glycerol) at 0 °C was placed in a prewarmed 96-well plate at 37 °C in the presence of tested compounds at varying concentrations. The reaction was started by warming the samples at 37 °C. The mass of polymer formed was monitored by turbidimetry at 340 nm every 1 min for 60 min with a BioTek's Synergy 4 multifunction microplate reader.

4.2.3. Cell cycle analysis

For flow cytometric analysis of DNA content, 10⁶ LOVO cells were treated with varying concentrations of compound **10** for 24 h. After centrifugation, the cell pellet was fixed in 2 ml citrate buffer. Fixed cells were treated with 1.5 ml RNase A for 20 min and afterwards stained with 1.5 ml propidium iodide for 20 min. Samples were analyzed on a BD FACStar Plus Cell Sorter Flow Cytometer, which was also used to determine the percentage of cells in the different phases of the cell cycle.

4.3. Molecular docking

All calculations were performed on an Origin 300 Server. The X-ray crystal structure of the DAMA-colchicine-tubulin complex

(PDB code 1SA0) was used as the tubulin protein template. The AutoDock program was used.¹⁹ A grid of 45 × 40 × 40 was used to ensure that the area probed was adequate for the ligands to explore all possible binding modes. Docking runs were performed using the Lamarckian genetic algorithm (LGA) with some modifications of the docking parameters. Each docking experiment was derived from 50 different runs that was set to terminate after a maximum of 10,000,000 energy evaluations or 370,000 generations, yielding 50 docked conformations. At the end of a docking job with multiple runs, AutoDock performed cluster analysis. Docking solutions with ligand all-atom RMSDs within 0.5 Å of each other were clustered together and ranked by the lowest energy representative. Low energy binding modes and the lowest energy conformation from clusters of five or more occurrences were selected for further refinement. These were then refined by Sybyl,²⁰ with the binding mode that had the lowest complex energy after minimisation being selected as the final binding mode.

Acknowledgments

The work was supported by the Key Program for Basic Research of Shanghai 'Technology Innovation Action Plan' (Grant No. 09JC1417500), Shanghai Natural Science Foundation (Grant No. 09ZR1438800) and National Natural Science Foundation of China (Grant No. 30901859).

Supplementary data

Supplementary data associated with this article can be found, in the online version, at doi:10.1016/j.bmc.2011.03.068.

References and notes

- Jordan, M. A.; Wilson, L. *Nat. Rev. Cancer* **2004**, *4*, 253.
- Nam, N. H. *Curr. Med. Chem.* **2003**, *10*, 1697.
- Tozer, G. M.; Kanthou, C.; Baguley, B. C. *Nat. Rev. Cancer* **2005**, *5*, 423.
- Chaudhary, A.; Pandeya, S. N.; Kumar, P.; Sharma, P. P.; Gupta, S.; Soni, N.; Verma, K. K.; Bhardwaj, G. *Mini-Rev. Med. Chem.* **2007**, *7*, 1186.
- Tron, G. C.; Pirali, T.; Sorba, G.; Pagliai, F.; Busacca, S.; Genazzani, A. A. *J. Med. Chem.* **2006**, *49*, 3033.
- Srivastava, V.; Negi, A. S.; Kumar, J. K.; Gupta, M. M.; Khanuja, S. P. S. *Bioorg. Med. Chem.* **2005**, *13*, 5892.
- Provot, O.; Giraud, A.; Peyrat, J. F.; Alami, M.; Brion, J. D. *Tetrahedron Lett.* **2005**, *46*, 8547.
- Lawrence, N. J.; Patterson, R. P.; Ooi, L. L.; Cook, D.; Ducki, S. *Bioorg. Med. Chem. Lett.* **2006**, *16*, 5844.
- Kerr, D. J.; Hamel, E.; Jung, M. K.; Flynn, B. L. *Bioorg. Med. Chem.* **2007**, *15*, 3290.
- Romagnoli, R.; Baraldi, P. G.; Carrion, M. D.; Cara, C. L.; Cruz-Lopez, O.; Preti, D.; Tolomeo, M.; Grimaudo, S.; Cristina, A. D.; Zonta, N.; Balzarini, J.; Sarkare, T.; Brancal, A.; Hamel, E. *Bioorg. Med. Chem.* **2008**, *16*, 5367.
- Kaffy, J.; Pontikis, R.; JFlorent, J. C.; Monneret, C. *Org. Biomol. Chem.* **2005**, *3*, 2657.
- Ty, N.; Kaffy, J.; Arrault, A.; Thoret, S.; Pontikis, R.; Dubois, J.; Morin-Allory, L.; Florent, J. C. *Bioorg. Med. Chem. Lett.* **2009**, *19*, 1318.
- Li, Y. N.; Li, Y. W.; Zheng, C. H.; Lv, J. G.; Tang, H.; Zhang, J.; Zhou, Y. J. *Yaoxue Shijian Zhazhi* **2008**, *26*, 447.
- Romagnoli, R.; Baraldi, P. G.; Pavani, M. G.; Tabrizi, M. A.; Preti, D.; Fruttarolo, F.; Piccagli, L.; Jung, M. K.; Hamel, E.; Borgatti, M.; Gambari, R. *J. Med. Chem.* **2006**, *49*, 3906.
- Romagnoli, R.; Baraldi, P. G.; Remusat, V.; Carrion, M. D.; Cara, C. L.; Preti, D.; Fruttarolo, F.; Pavani, M. G.; Tabrizi, M. A.; Tolomeo, M.; Grimaudo, S.; Balzarini, J.; Jordan, M. A.; Hamel, E. *J. Med. Chem.* **2006**, *49*, 6425.
- Bailly, C.; Bal, C.; Barbier, P.; Combes, S.; Finet, J. P.; Hildebrand, M. P.; Peyrot, V.; Watzet, N. *J. Med. Chem.* **2003**, *46*, 5437.
- Hamel, E. *Cell Biochem. Biophys.* **2003**, *38*, 1.
- Zhang, Q.; Peng, Y.; Wang, X. I.; Keenan, S. M.; Arora, S.; Welsh, W. J. *J. Med. Chem.* **2007**, *50*, 749.
- Morris, G. M.; Goodsell, D. S.; Halliday, R. S.; Huey, R.; Hart, W. E.; Belew, R. K.; Olson, A. J. *J. Comput. Chem.* **1998**, *19*, 1639.
- SYBYL, release version 6.9; Tripos Associates, St. Louis, Missouri.